

Matrix Models of Induced Large- N QCD

Yu. Makeenko¹

*Institute of Theoretical and Experimental Physics
B.Cheremuskinskaya 25, 117259 Moscow*

Abstract

I review recent works on the problem of inducing large- N QCD by matrix fields. In the first part of the talk I describe the matrix models which induce large- N QCD and present the results of studies of their phase structure by the standard lattice technology (in particular, by the mean field method). The second part is devoted to the exact solution of these models in the strong coupling region by means of the loop equations.

Talk at the Seminar on Strings, Matrix Models and all that, Rakhov, FSU, October 1992.

¹E-mail: makeenko@vxitep.itep.msk.su / makeenko@desyvax.bitnet / makeenko@nbivax.nbi.dk

1 Introduction

Recently there has renewed interest in the problem of inducing QCD by means of some pre-theory. As was proposed by Kazakov and Migdal [1], such a theory can be potentially solvable in the limit of large number of colors, N_c , providing the inducing model is that of the (self-interacting) matrix scalar field in the *adjoint* representation of the gauge group $SU(N_c)$ on the lattice. The gauge field is attached in the usual way to make the model gauge invariant except no kinetic term for the gauge field. The latter circumstance differs the Kazakov–Migdal model from the standard lattice Higgs–gauge models. It was conjectured in Ref. [1] that the model undergoes, with decreasing the bare mass of the scalar field, a second order phase transition which is associated with continuum QCD when the critical point is approached from the strong coupling region.

To solve the Kazakov–Migdal model in the strong coupling region, Migdal [2] applied the Riemann–Hilbert method and derived the master field equation to determine the $N_c = \infty$ solution. An explicit solution of this equation for the quadratic potential is found by Gross [3]. A surprising property of the master field equation (not yet completely understood) is that it admits [2, 4] self-consistent scaling solutions with non-trivial critical indices for the non-quadratic potentials. Moreover, the very Riemann–Hilbert method of Ref. [2] was developed, in fact, to find such a scaling solution.

These nice features of the Kazakov–Migdal model are due to the fact that the scalar field is in the adjoint representation of the gauge group. For this reason it can be diagonalized by a (local) gauge transformation so that only $\mathcal{O}(N_c)$ degrees of freedom are left and the saddle-point method is applicable as $N_c \rightarrow \infty$. However, a price for having the adjoint-representation field is an extra local Z_N symmetry which leads [5] at $N_c = \infty$ to *local confinement* (*i.e.* the infinite string tension) rather than area law for the Wilson loops.

In the present talk I review the papers [6, 7, 8] where the questions of which models induce large- N_c QCD with normal area and how to solve these models in the strong coupling region were answered². In Sect. 2 I describe the models, both scalar and fermion ones, which induce large- N_c QCD. The mechanism exploited is based on the first order phase transition which occurs with decreasing bare mass of the inducing field and is associated with freezing the gauge field and the restoration of area law. In Sect. 3 I discuss the exact strong coupling solution for the quadratic potential, both in scalar and in fermion cases. It is obtained by solving loop equations which turn out to be a useful tool for studies of the matrix models.

²For a review of other approaches, see recent surveys [9, 10, 11] and references therein

2 The models of induced large- N QCD

Since the inducing matter field is in the adjoint representation of $SU(N_c)$, Wilson loops vanish to each order of the large mass expansion at $N_c = \infty$. This situation is associated with local confinement. However, the area law is restored with decreasing bare mass at the point of the first order large- N_c phase transition. Its existence can be rigorously proven for the single-plaquette adjoint action and is expected for more complicated models on the basis of the mean field method. Once the first order phase transition occurs, the proper model will induce large- N_c QCD in the continuum.

2.1 Adjoint scalar model

A simplest way to induce large- N_c QCD is by adjoint representation scalars at N_f flavors (*i.e.* the number of different species). The *adjoint scalar model* ASM is defined by the partition function

$$Z_{ASM} = \int \prod_{x,\mu} dU_\mu(x) \prod_x \prod_{f=1}^{N_f} d\Phi_f(x) e^{\sum_{f=1}^{N_f} \sum_x N_c \text{tr} \left(-V[\Phi_f(x)] + \sum_{\mu=1}^D \Phi_f(x) U_\mu(x) \Phi_f(x+\mu) U_\mu^\dagger(x) \right)}$$
(2.1)

where the fields $\Phi_f(x)$ ($f = 1, \dots, N_f$) take values in the adjoint representation of the gauge group $SU(N_c)$ and the link variable $U_\mu(x)$ belongs to the gauge group. The potential $V[\Phi]$ is given by

$$V[\Phi] = \frac{m}{2} \Phi^2 + \dots$$
(2.2)

where m is the (square of the) bare mass of the scalar field. The original Kazakov–Migdal model [1] corresponds to $N_f = 1$. Notice that the action in Eq. (2.1) is diagonal w.r.t. the flavor indices.

The case of $N_f = 1$ is a unique one when the matrix $\Phi(x)$ can be reduced to a diagonal form at each site of the lattice by means of a gauge transformation. Only at $N_f = 1$ the Riemann-Hilbert method of Ref. [2] is therefore applicable. The alternative method of solving ASM with the quadratic potential at strong coupling is based on loop equations [7] and can be used at any N_f while gives at $N_f = 1$ the same result as the Riemann–Hilbert method.

It is worth noting that one can integrate in (2.1) over arbitrary hermitean matrices rather than over those in the adjoint representation which gives at finite N_c a different model for the case of a non-quadratic potential. These two models should coincide, however, as $N_c \rightarrow \infty$.

2.2 Adjoint fermion model

An alternative to ASM is the *adjoint fermion model* (AFM) which is defined by the partition function

$$Z_{AFM} = \int \prod_{x,\mu} dU_\mu(x) \prod_x \prod_{f=1}^{N_f} d\Psi_f(x) d\bar{\Psi}_f(x) e^{-S_F[\Psi, \bar{\Psi}, U]}. \quad (2.3)$$

Here $S_F[\Psi, \bar{\Psi}, U]$ is the lattice fermion action

$$S_F[\Psi, \bar{\Psi}, U] = \sum_{f=1}^{N_f} \sum_x N_c \text{tr} \left(V_{\text{even}}(\bar{\Psi}_f(x) \Psi_f(x)) - \sum_{\mu=1}^D [\bar{\Psi}_f(x) P_\mu^- U_\mu(x) \Psi_f(x + \mu) U_\mu^\dagger(x) + \bar{\Psi}_f(x + \mu) P_\mu^+ U_\mu^\dagger(x) \Psi_f(x) U_\mu(x)] \right) \quad (2.4)$$

where

$$V_{\text{even}}(\bar{\Psi}\Psi) = m\bar{\Psi}\Psi + \dots \quad (2.5)$$

is a fermionic analogue of the potential (2.2) and m is the bare mass of the fermion field.

In Eqs. (2.3), (2.4) $\Psi_f(x)$ is the Grassmann anticommuting $N_c \times N_c$ matrix field while

$$P_\mu^\pm = r \pm \gamma_\mu \quad (2.6)$$

stand for the projectors. The case $r = 0$ corresponds to chiral fermions while $r = 1$ is associated with Wilson fermions. As is well known, the chiral fermions describe $2^D N_f$ flavors in the naive continuum limit while Wilson fermions are associated with N_f flavors.

2.3 The induced action

The above matrix models can be represented in the form of a *gauge theory* given by the partition function

$$Z = \int \prod_{x,\mu} dU_\mu(x) e^{-S_{\text{ind}}[U_\mu(x)]}, \quad (2.7)$$

where the *induced action* for the gauge field $U_\mu(x)$ is defined by the integral over $\Phi(x)$ in Eq. (2.1) or over $\Psi(x)$ and $\bar{\Psi}(x)$ in Eq. (2.3):

$$e^{-S_{\text{ind}}[U_\mu(x)]} = \int \prod_x \prod_{f=1}^{N_f} d\Phi_f(x) e^{\sum_{f=1}^{N_f} \sum_x N_c \text{tr} \left(-V[\Phi_f(x)] + \sum_{\mu=1}^D \Phi_f(x) U_\mu(x) \Phi_f(x + \mu) U_\mu^\dagger(x) \right)} \quad (2.8)$$

or

$$e^{-S_{\text{ind}}[U_\mu(x)]} = \int \prod_x \prod_{f=1}^{N_f} d\Psi_f(x) d\bar{\Psi}_f(x) e^{-S_F[\Psi, \bar{\Psi}, U]}, \quad (2.9)$$

with $S_F[\Psi, \bar{\Psi}, U]$ given by Eq. (2.4).

For the quadratic potential the result of integrating over $\Phi(x)$ or over $\Psi(x)$ and $\bar{\Psi}(x)$ is given by the large mass expansion:

$$S_{ind}[U] = -\frac{N_f}{2} \sum_{\Gamma} \frac{|\text{tr } U(\Gamma)|^2}{l(\Gamma)} \left(\frac{2}{m}\right)^{l(\Gamma)} \quad (2.10)$$

for scalars or

$$S_{ind}[U] = -N_f \sum_{\Gamma} \frac{|\text{tr } U(\Gamma)|^2}{l(\Gamma)m^{l(\Gamma)}} \text{Sp} \prod_{l \in \Gamma} P_{\mu}^{\pm} \quad (2.11)$$

for fermions. In Eq. (2.11) Sp stands for the trace over the spinor indices of the path-ordered product of the projectors (2.6) (plus or minus depends on the orientation of the link l) along the loop Γ .

One easily sees that only single plaquettes survive in the sum over path on the r.h.s.'s of Eqs. (2.10) and (2.11) if $m \sim N_f^{1/4}$ as $N_f \rightarrow \infty$, so that the single plaquette adjoint action arises in the large- N_f limit:

$$S_A = -\frac{\beta_A}{2} \sum_p |\text{tr } U(\partial p)|^2 \quad (2.12)$$

with

$$\begin{aligned} \beta_A &= \frac{4N_f}{m^4} && \text{for scalars;} \\ \beta_A &= \frac{2^{\frac{D}{2}-1} N_f (1 + 2r^2 - r^4)}{m^4} && \text{for fermions.} \end{aligned} \quad (2.13)$$

This shows of how ASM and AFM induce the single plaquette lattice gauge theory with adjoint action.

2.4 The large- N phase transition

The inducing of large- N_c QCD relies on the fact [12] that the lattice gauge theory defined by the partition function (2.7) with the action (2.12) undergoes the first order large- N_c phase transition at $\beta_A \approx 2$ after which the gauge field $U_{\mu}(x)$ becomes frozen near some mean-field value η ($\eta \rightarrow 1$ as $\beta_A \rightarrow \infty$).

The proof of the existence of the phase transition is based solely on the factorization at large- N_c which says that the adjoint action (2.12) is equivalent at $N_c = \infty$ to the single-plaquette *fundamental* action

$$S_F[U] = N_c \bar{\beta} \sum_p \Re \text{tr } U(\partial p) \quad (2.14)$$

providing the coupling $\bar{\beta}$ is determined by

$$\bar{\beta} = \beta_A W_F(\partial p; \bar{\beta}) \quad (2.15)$$

where $W_F(\partial p; \bar{\beta})$ stands for the plaquette average

$$W_F(\partial p; \bar{\beta}) \equiv \frac{\int \prod_{x,\mu} dU_\mu(x) e^{-S_F[U]} \frac{1}{N_c} \text{tr} U(\partial p)}{\int \prod_{x,\mu} dU_\mu(x) e^{-S_F[U]}}. \quad (2.16)$$

Eq. (2.15) can be naively obtained substituting one of two traces in the action (2.12) by the average. A rigorous proof [12] is based on the loop equations.

The existence of the first order phase transition for the action (2.12) with decreasing β_A can be seen as follows. Let us solve Eq. (2.15) for $\bar{\beta}(\beta_A)$ substituting for (2.16) the strong coupling expansion

$$W_F(\partial p; \bar{\beta}) = \frac{\bar{\beta}}{2} + \frac{\bar{\beta}^5}{8} \quad \text{at strong coupling}. \quad (2.17)$$

Eq. (2.15) possesses at any $\bar{\beta}$ a trivial solution $\bar{\beta} = 0$. However, one more solution appears for $\bar{\beta} \approx 2$:

$$\bar{\beta} \propto \left(\frac{1}{2} - \frac{1}{\beta_A} \right)^{\frac{1}{4}}, \quad (2.18)$$

which matches the weak coupling solution

$$\bar{\beta} \rightarrow \beta_A - \frac{1}{4} \quad \text{as} \quad \beta_A \rightarrow \infty. \quad (2.19)$$

Notice that $\bar{\beta} \ll 1$ for the solution (2.18) when $\beta_A \approx 2$ so that the strong coupling expansion is applicable.

The adjoint plaquette average

$$W_A(\partial p; \beta_A) \equiv \frac{\int \prod_{x,\mu} dU_\mu(x) e^{-S_A[U]} \frac{1}{N_c^2} \left(|\text{tr} U(\partial p)|^2 - 1 \right)}{\int \prod_{x,\mu} dU_\mu(x) e^{-S_A[U]}} \quad (2.20)$$

which is given due to the factorization by

$$W_A(\partial p; \beta_A) = \left(W_F(\partial p; \bar{\beta}) \right)^2 = \left(\frac{\bar{\beta}}{\beta_A} \right)^2 \quad (2.21)$$

is depicted in Fig. 1. Since the slope is negative for the solution (2.18) near $\beta_A = 2$, a first order phase transition must occur with increasing β_A . This negative slope is a consequence solely of the positive sign of the second term on the r.h.s. of Eq. (2.17). The predicted value of the critical coupling β_A^* , at which the phase transition occurs, obeys $\beta_A^* < 2$, as is seen from Fig. 1, to be compared with the result of Monte-Carlo simulations $\beta_A^* = 1.7 - 1.8$.

2.5 The mean field phase diagram

At finite N_f the induced actions (2.10) or (2.11) can not be exactly analyzed even at $N_c = \infty$. An approximate mean field method, which usually works very well in the cases of first order phase transitions, was applied to obtain the phase diagram in Refs. [6, 8].

Naively, the mean field approximation consists in substituting the link variable $U_\mu(x)$ by the mean field value

$$[U_\mu(x)]^{ij} = \eta \delta^{ij} \quad (2.22)$$

everywhere but one link and writing a self-consistency condition at this link. The self-consistency condition is given by the one-link problem

$$\eta^2 = \frac{\int dU e^{\frac{b_A}{2} |\text{tr} U|^2} \frac{1}{N^2} |\text{tr} U|^2}{\int dU e^{\frac{b_A}{2} |\text{tr} U|^2}} \quad (2.23)$$

where

$$b_A = \frac{\int \prod_x d\Phi(x) e^{\sum_x N \text{tr} \left(-V[\Phi(x)] + \eta^2 \sum_\mu \Phi(x) \Phi(x+\mu) \right)} \frac{1}{N} \text{tr} \Phi(0) \Phi(0+\mu)}{\int \prod_x d\Phi(x) e^{\sum_x N \text{tr} \left(-V[\Phi(x)] + \eta^2 \sum_\mu \Phi(x) \Phi(x+\mu) \right)}}. \quad (2.24)$$

These naive mean field formulas can be obtained [6] in the framework of the variational method.

The mean field phase diagram which was obtained by an analysis of Eqs. (2.23) and (2.24) is depicted in Fig. 2. At $N_f = 1$ there is no first order phase transition for the quadratic potential in the stability region $m > 2D$. For $m < 2D$ the model is unstable and were in the Higgs phase if the stabilizing higher order in Φ terms would be added to the potential (2.2). The desired large- N_c phase transition appears for $N_f > N_f^* \approx 30$.³ ASM looks in this region exactly like the single-plaquette adjoint model discussed in the previous subsection.

A similar phase diagram for AFM is depicted in Fig. 3. Now there is no Higgs phase (or an instability region for the quadratic potential) due to the fermionic nature of inducing fields. For the cases of chiral and Kogut–Susskind fermions the first order phase transition is present already for $N_f = 1$ while the result for Wilson fermions is less certain.

2.6 Area law versus local confinement

At the point of the first order large- N_c phase transition, the area law behavior of the (adjoint) Wilson loops which is associated with normal confinement is restored in ASM or AFM analogously to the single-plaquette adjoint action [12].

In order to see this, let us consider the adjoint Wilson loop which is defined by

$$W_A(C) = \left\langle \frac{1}{N_c^2} \left(|\text{tr} U(C)|^2 - 1 \right) \right\rangle \quad (2.25)$$

where the average is understood w.r.t. the same measure as in Eq. (2.1) or in Eq. (2.3). Alternatively, one can average w.r.t. the induced actions (2.10) (2.11) which recovers at

³Such a phase diagram is compatible with the Monte–Carlo studies of Ref. [13].

$N_f = \infty$ the single plaquette adjoint action (2.12). In this limiting case the following extension of the factorization formula (2.21) holds at $N_c = \infty$:

$$W_A(C; \beta_A) = \left(W_F(C; \bar{\beta}) \right)^2, \quad (2.26)$$

where $W_F(C; \bar{\beta})$ is defined by the same formula as (2.16) with ∂p replaced by an arbitrary contour C and $\bar{\beta}$ versus β_A given by Eq. (2.15).

Since $\bar{\beta} = 0$ for $\beta_A < \beta_A^*$, $W_A(C)$ vanishes in this region due to Eq. (2.26) except the loops with vanishing minimal area $A_{min}(C)$:

$$W_A(C) = \delta_{0A_{min}(C)} + \mathcal{O}\left(\frac{1}{N_c^2}\right). \quad (2.27)$$

On the contrary, the area law with the string tension

$$K_A(\beta_A) = 2 K_F(\bar{\beta}(\beta_A)) \quad (2.28)$$

holds for $\beta_A > \beta_A^*$ when Eq. (2.15) possesses the non-trivial solution. An extension of these formulas to finite N_f is given in Ref. [7].

While the first order phase transition associated with the restoration of area law looks similar for ASM and AFM, the continuum limits should be approached in different ways. For ASM the continuum QCD is reached at the line of second order phase transitions which separates the area law and Higgs phases provided that one approaches it from the area law phase. For AFM there is no Higgs phase and continuum QCD is reached as $m \rightarrow 0$.

3 Loop equations at strong coupling

The loop equations of ASM or AFM relate the closed adjoint Wilson loop (2.25) to the open ones with scalars or fermions at the ends. The loop equations are drastically simplified at $N_c = \infty$ in the strong coupling region where the closed loops obey Eq. (2.27). The exact solution can be obtained in both cases for the quadratic potential when the loop equations turns out to be equivalent to those for the hermitean and complex one-matrix models, respectively.

3.1 Loop equations for arbitrary potential

The generic object which appear in the loop equations are open Wilson loops

$$\delta_{ff'} G_\lambda(C_{xy}) = \left\langle \frac{1}{N_c} \text{tr} \left(\Phi_f(x) U(C_{xy}) \frac{1}{\lambda - \Phi_{f'}(y)} U^\dagger(C_{xy}) \right) \right\rangle. \quad (3.1)$$

The appearance of the δ -symbol w.r.t. the flavor indices f and f' is due to the fact that the interaction terms in the action entering Eq. (2.1) are diagonal over the flavor indices.

The loop equations of ASM result from the invariance of the measure in Eq. (2.1) under an arbitrary shift of $\Phi_f(x)$ and reads

$$\begin{aligned} & \left\langle \frac{1}{N_c} \text{tr} \left(V'(\Phi_f(x)) U(C_{xy}) \frac{1}{\lambda - \Phi_{f'}(y)} U^\dagger(C_{xy}) \right) \right\rangle \\ & - \sum_{\substack{\mu=-D \\ \mu \neq 0}}^D \left\langle \frac{1}{N_c} \text{tr} \left(\Phi_f(x + \mu) U(C_{(x+\mu)x} C_{xy}) \frac{1}{\lambda - \Phi_{f'}(y)} U^\dagger(C_{(x+\mu)x} C_{xy}) \right) \right\rangle = \\ & \cdot \delta_{ff'} \delta_{xy} \left\langle \frac{1}{N_c} \text{tr} \left(U(C_{xy}) \frac{1}{\lambda - \Phi_f(y)} \right) \frac{1}{N_c} \text{tr} \left(\frac{1}{\lambda - \Phi_f(y)} U^\dagger(C_{xy}) \right) \right\rangle \end{aligned} \quad (3.2)$$

where the path $C_{(x+\mu)x} C_{xy}$ on the l.h.s. is obtained by attaching the link (x, μ) to the path C_{xx} at the end point x as is depicted in Fig. 4. I have omitted additional contact terms which arise at finite N_c due to the fact that Φ belongs to the adjoint representation, so that Eq. (3.2) is written for the hermitean matrices. This difference disappears, however, as $N_c \rightarrow \infty$.

The analogues of Eqs. (3.1) and (3.2) for AFM read

$$\delta_{ff'} G_\lambda^{ij}(C_{xy}) = \left\langle \frac{1}{N_c} \text{tr} \left(\Psi_f^i(x) U(C_{xy}) \frac{\lambda \bar{\Psi}_{f'}^j(y)}{\lambda^2 - \bar{\Psi}_{f'}(y) \Psi_{f'}(y)} U^\dagger(C_{xy}) \right) \right\rangle \quad (3.3)$$

where i and j are spinor indices, and

$$\begin{aligned} & \left\langle \frac{1}{N_c} \text{tr} \left(\Psi_f(x) V'_{\text{even}}(\bar{\Psi}_f(x) \Psi_f(x)) U(C_{xy}) \frac{\bar{\Psi}_f(x)}{\lambda - \bar{\Psi}_f(x) \Psi_{f'}(y)} U^\dagger(C_{xy}) \right) \right\rangle \\ & - \sum_{\mu=1}^D \left\langle \frac{1}{N_c} \text{tr} \left(P_\mu^+ \Psi_f(x + \mu) U(C_{(x+\mu)x} C_{xy}) \frac{\lambda \bar{\Psi}_{f'}(y)}{\lambda - \bar{\Psi}_{f'}(y) \Psi_{f'}(y)} U^\dagger(C_{(x+\mu)x} C_{xy}) \right. \right. \\ & \quad \left. \left. + P_\mu^- \Psi_f(x - \mu) U(C_{(x-\mu)x} C_{xy}) \frac{\lambda \bar{\Psi}_{f'}(y)}{\lambda - \bar{\Psi}_{f'}(y) \Psi_{f'}(y)} U^\dagger(C_{(x-\mu)x} C_{xy}) \right) \right\rangle \\ & = \delta_{ff'} \delta_{xy} \left\langle \frac{1}{N_c} \text{tr} \left(U(C_{xy}) \frac{\lambda}{\lambda^2 - \bar{\Psi}_f(y) \Psi_f(y)} \right) \frac{1}{N_c} \text{tr} \left(\frac{\lambda}{\lambda^2 - \bar{\Psi}_f(y) \Psi_f(y)} U^\dagger(C_{xy}) \right) \right\rangle. \end{aligned} \quad (3.4)$$

The matrix multiplication over the spinor indices is implied in this equation.

3.2 Loop equations at large N_c

The path C_{xy} on the r.h.s. of Eq. (3.2) (or Eq. (3.4)) is always closed due to the presence of the delta-function. The explicit equation for the case of vanishing (or contractable) contour $C_{xx} = 0$ at large N_c , when the factorization holds, reads

$$\int_{C_1} \frac{d\omega}{2\pi i} \frac{V'(\omega)}{(\lambda - \omega)} E_\omega - 2DG_\lambda(1) = E_\lambda^2 \quad (3.5)$$

where

$$E_\lambda \equiv \left\langle \frac{1}{N_c} \text{tr} \left(\frac{1}{\lambda - \Phi_f(x)} \right) \right\rangle = \frac{1}{\lambda} (G_\lambda(0) + 1) \quad (3.6)$$

with G_λ is defined by Eq. (3.1). I have denoted the one-link average by

$$G_\lambda(1) = G_\lambda(C_{(x\pm\mu)x}) \quad (3.7)$$

since the r.h.s. does not depend on x and μ due to the invariance under translations by a multiple of the lattice spacing and/or rotations by a multiple of $\pi/2$ on the lattice. The contour C_1 encircles singularities of E_ω so that the integration over ω on the l.h.s. of Eq. (3.5) plays the role of a projector picking up negative powers of λ .

For $C_{xx} \neq 0$, the averages of a new kind arise on the r.h.s. of Eq. (3.2) (or Eq. (3.4)). However, these averages obey at $N_c = \infty$ the following analogue of Eq. (2.27)

$$\left\langle \frac{1}{N_c} \text{tr} \left(U(C_{xx}) \frac{1}{\lambda - \Phi_f(x)} \right) \frac{1}{N_c} \text{tr} \left(U^\dagger(C_{xx}) \frac{1}{\lambda - \Phi_f(x)} \right) \right\rangle = \delta_{0, A_{\min}(C)} E_\lambda^2 + \mathcal{O} \left(\frac{1}{N_c^2} \right) \quad (3.8)$$

i.e. vanish for $C_{xx} \neq 0$.

Hence, the loop equation for $C_{xy} \neq 0$ at $N_c = \infty$ reads

$$\left\langle \frac{1}{N_c} \text{tr} \left(V'(\Phi_f(x)) U(C_{xy}) \frac{1}{\lambda - \Phi_{f'}(y)} U^\dagger(C_{xy}) \right) \right\rangle - \sum_{\substack{\mu=-D \\ \mu \neq 0}}^D G_\lambda(C_{(x+\mu)x} C_{xy}) = 0 \quad (3.9)$$

independently of whether C_{xy} is closed or open. Therefore, the r.h.s. of the loop equation in nonvanishing at $N_c = \infty$ only for $C_{xy} = 0$ (modulo backtrackings) when the proper equation is given by Eq. (3.5).

Finally, the fermionic analogues of Eqs. (3.8) and (3.6) read

$$\left\langle \frac{1}{N_c} \text{tr} \left(U(C_{xx}) \frac{\lambda}{\lambda^2 - \bar{\Psi}_f(x) \Psi_f(x)} \right) \frac{1}{N_c} \text{tr} \left(U^\dagger(C_{xx}) \frac{\lambda}{\lambda^2 - \bar{\Psi}_f(x) \Psi_f(x)} \right) \right\rangle = \delta_{0, A_{\min}(C)} E_\lambda^2 + \mathcal{O} \left(\frac{1}{N_c^2} \right) \quad (3.10)$$

and

$$E_\lambda = \left\langle \frac{1}{N_c} \text{tr} \left(\frac{\lambda}{\lambda^2 - \bar{\Psi}_f(x) \Psi_f(x)} \right) \right\rangle = \frac{1}{\lambda} (G_\lambda^{ii}(0) + 1) \quad (3.11)$$

with G_λ defined by Eq. (3.3). Therefore, the r.h.s. of Eq. (3.4) involves at $N_c = \infty$ only E_λ similarly to the scalar case.

3.3 The quadratic potential

The quadratic potential is always solvable, even in the non-diagonalizable cases, for the following reasons. Let us consider the one-link correlator

$$\left\langle \frac{1}{N_c} \text{tr} t^a U \chi_{f'} U^\dagger \right\rangle_U \equiv \frac{\int dU e^{N_c \sum_f \varphi_f U \chi_f U^\dagger} \frac{1}{N_c} \text{tr} t^a U \chi_{f'} U^\dagger}{\int dU e^{N_c \sum_f \varphi_f U \chi_f U^\dagger}} \quad (3.12)$$

where t_a ($a = 1, \dots, N_c^2 - 1$) stand for generators of $SU(N_c)$ which are normalized by

$$\frac{1}{N_c} \text{tr } t^a t^b = \delta^{ab}. \quad (3.13)$$

At $N_c = \infty$ the formula

$$\left\langle \frac{1}{N_c} \text{tr } t^a U \chi_{f'} U^\dagger \right\rangle_U = \Lambda \frac{1}{N_c} \text{tr } t^a \varphi_{f'}, \quad (3.14)$$

where Λ is a constant to be determined below, can be proven for φ and χ given by the master field for the quadratic potential analyzing the large mass expansion. The point is that terms like $\text{tr } t^a \varphi_{f'}^k$, with $k > 1$ never appear for the quadratic potential. Analogously it can be proven that

$$\left\langle \frac{1}{N_c} \text{tr } t^a U \frac{1}{\lambda - \chi_{f'}} U^\dagger \right\rangle_U = \Lambda \frac{1}{N_c} \text{tr } t^a \frac{1}{\lambda - \varphi_{f'}}. \quad (3.15)$$

For $N_f = 1$ Eqs. (3.14) and (3.15) recovers the ones of Ref. [14].

For $G_\lambda(C_{xy})$ defined by Eq. (3.1), Eq. (3.15) implies

$$G(C_{xy}) = \Lambda^L E_\lambda \quad (3.16)$$

where L is the *algebraic* length (*i.e.* the one after contracting the backtrackings) of C_{xy} . The fermionic analogue of this formula reads

$$G_\lambda^{ij}(C_{xy}) = \Lambda^L E_\lambda \left(\prod_{l \in C_{xy}} P_\mu^\pm \right)^{ij} \quad (3.17)$$

where the plus or minus signs correspond to the direction of the link l which belongs to the contour C_{xy} . The spin factor will provide below the cancellation of the projectors in Eq. (3.4).

The constant Λ can be determined by substituting the ansatz (3.16) into the $C_{xy} \neq 0$ loop equation (3.9) which simplifies for the quadratic potential as [7]

$$m G_\lambda(C_{xy}) - \sum_{\substack{\mu=-D \\ \mu \neq 0}}^D G_\lambda(C_{(x+\mu)x} C_{xy}) = 0. \quad (3.18)$$

The ansatz (3.16) satisfies this equation for any $C_{xy} \neq 0$ providing

$$\Lambda = \frac{2}{m + \sqrt{m^2 + 4(1 - 2D)\sigma}} \quad (3.19)$$

where $\sigma = 1$ for scalars or

$$\sigma = P_\mu^+ P_\mu^- = r^2 - 1 \quad (3.20)$$

for fermions ($\sigma = -1$ for chiral fermions and $\sigma = 0$ for Wilson fermions).

The remaining function E_λ can now be determined from Eq. (3.5) which for the quadratic potential reads

$$\tilde{m}E_\lambda = E_\lambda^2, \quad \tilde{m} = m - 2D\Lambda \quad (3.21)$$

and coincides with the loop equation for the Gaussian hermitean one-matrix model (for a review, see Ref. [15] and references therein). The solution of Eq. (3.21) which satisfies

$$E_\lambda \rightarrow \frac{1}{\lambda} \quad \text{as } \lambda \rightarrow \infty, \quad (3.22)$$

as it should be due to the definition (3.6), is unambiguous:

$$2E_\lambda = \tilde{m}\lambda - \tilde{m}\sqrt{\lambda^2 - 4/\tilde{m}}. \quad (3.23)$$

The imaginary part

$$\Im E_\lambda \equiv \rho(\lambda) = \frac{1}{4\pi}\tilde{m}\sqrt{4/\tilde{m} - \lambda^2} \quad \text{for } -2/\sqrt{\tilde{m}} \leq \lambda \leq 2/\sqrt{\tilde{m}} \quad (3.24)$$

recovers the solution [3]. Analogously, the $C_{xx} = 0$ loop equation for AFM with the quadratic potential is reduced to the loop equation for the complex one-matrix model [15].

One should not be surprised that the exact strong coupling solution for the quadratic potential does not depend on N_f which is a consequence of the peculiar behavior of the Wilson loops (2.27). This independence does not contradict to the fact that the first order phase transition discussed in Sect. 2 occurs only for $N_f > N_f^*$. The point is that the strong coupling solution is not sensitive to the phase transition which occurs due to another (thermodynamic) reason.

3.4 Interpretation as the 1D tree problem

A question arises what combinatorial problem are the exact solutions of the previous subsection associated with? To answer, let us consider the open loop correlator

$$\delta_{ff'}G(C_{xy}) = \left\langle \frac{1}{N_c} \text{tr} \left(\Phi_f(x)U(C_{xy})\Phi_{f'}(y)U^\dagger(C_{xy}) \right) \right\rangle. \quad (3.25)$$

which is nothing but the λ^{-2} term of the expansion of (3.1) in λ^{-1} . At $N_c = \infty$ the standard sum-over-path representation of $G(C_{xy})$ reads

$$G(C_{xy}) = \sum_{\Gamma_{yx}} \left(\frac{2}{m} \right)^{l(\Gamma)+1} W_A(C_{xy}\Gamma_{yx}) \quad (3.26)$$

where the contour Γ_{yx} forms together with C_{cy} a closed loop passing x and y .

Since in our case the formula (2.27) associated with the infinite string tension holds, Γ_{yx} must coincide with $(C_{xy})^{-1}$ (*i.e.* passed in opposite direction) modulo backtrackings of Γ . Eq. (3.26) then yields

$$G(C_{xy}) = \sum_{\Gamma_{yx}} \left(\frac{2}{m}\right)^{l(\Gamma)+1} \quad (3.27)$$

where the sum goes over contours of the type depicted in Fig. 5.⁴

The fermionic analogues of Eqs. (3.25) to (3.27) read

$$G^{ij}(C_{xy}) = \sum_{\Gamma_{yx}} \left(\frac{1}{m}\right)^{l(\Gamma)+1} W_A(C_{xy}\Gamma_{yx}) \left(\prod_{l \in C_{xy}} P_\mu^\pm\right)^{ij} \quad (3.28)$$

and

$$G^{ii}(C_{xy}) = \sum_{\Gamma_{yx}} \left(\frac{1}{m}\right)^{l(\Gamma)+1} \text{Sp} \left(\prod_{l \in C_{xy}} P_\mu^\pm\right) \quad (3.29)$$

with summing again over contours depicted in Fig. 5.

The proper combinatorial problem is, therefore, that of summing over 1-dimensional trees embedded in a D -dimensional space. The exact solution of loop equations for the quadratic potential represents the solution to this problem:

$$G(C_{xy}) = \Lambda^L \frac{2D - 1}{m(D - 1) + D\sqrt{m^2 + 4(1 - 2D)\sigma}}, \quad (3.30)$$

where L is the algebraic length of C_{xy} and Λ is defined by Eq. (3.19). Such a dependence on Λ is evident from the representation (3.27) (or (3.29)) since the trees are uniformly distributed along C_{xy} .

As is already mentioned in the previous section, this solution coincides for scalars with that of Ref. [3]. Eq. (3.30) takes an especially simple form for Wilson fermions when the backtracking parameter σ , given by Eq. (3.20), vanishes so that there are no backtrackings. For chiral fermions when $\sigma = -1$ the solution (3.30) coincides with that of Ref. [16] for the case of the fundamental representation and vanishing constant in front of the plaquette term in the action. The point is that Wilson loops vanish in this case as well (except for those with vanishing minimal area) and exactly the same combinatorial problem of summing the diagrams of the type depicted in Fig. 5 emerges.

Acknowledgement

I am grateful to the theoretical physics department of the University of Zaragoza for the hospitality last December when the manuscript was being prepared for publication.

⁴One should not confuse the double lines in Fig. 5 which are due to backtrackings with the double lines in Fig. 4 which represent the adjoint representation.

References

- [1] V.A. Kazakov and A.A. Migdal, *Induced QCD at large N*, Paris / Princeton preprint LPTENS-92/15 / PUPT-1322 (June, 1992).
- [2] A.A. Migdal, *Exact solution of induced lattice gauge theory at large N*, Princeton preprint PUPT-1323 (June, 1992).
- [3] D. Gross, *Phys. Lett.* **293B** (1992) 181.
- [4] A.A. Migdal, *Phase transitions in induced QCD*, Paris preprint LPTENS-92/22 (August, 1992).
- [5] I.I. Kogan, G.W. Semenoff and N. Weiss, *Phys. Rev. Lett.* **69** (1992) 3435;
Yu. Makeenko, Talk at the Seminar on Strings, Matrix Models and all that, Kiev, June 1992.
- [6] S. Khokhlachev and Yu. Makeenko, *Phys. Lett.* **297B** (1992) 345.
- [7] Yu. Makeenko, *Large-N reduction, master field and loop equations in the Kazakov–Migdal model*, Moscow preprint ITEP-YM-6-92 (August, 1992), *Mod. Phys. Lett.* in press.
- [8] S. Khokhlachev and Yu. Makeenko, *Mod. Phys. Lett.* **A7** (1992) 3653.
- [9] V.A. Kazakov, *D-dimensional induced gauge theory as a solvable matrix model*, CERN-TH-6754/92 (December, 1992).
- [10] G.J. Gross, *Some new/old approaches to QCD*, LBL 33232, PUPT 1355 (November, 1992).
- [11] Talks by G. Semenoff and N. Wess at this Seminar.
- [12] S. Khokhlachev and Yu. Makeenko, *Phys. Lett.* **101B** (1981) 403; *ZhETF* **80** (1981) 448 (Sov. Phys. JETP **53** (1981) 228).
- [13] A. Gocksch and Y. Shen, *Phys. Rev. Lett.* **69** (1992) 2747;
S. Aoki, A. Gocksch and Y. Shen, *A study of the $N = 2$ Kazakov–Migdal model*, preprint UTHEP-242 (August, 1992).
- [14] A.A. Migdal, *Mixed model of induced QCD*, Paris preprint LPTENS-92/23 (August, 1992).
- [15] Yu. Makeenko, *Mod. Phys. Lett.* **A6** (1991) 1901.
- [16] H. Klugberg-Stern, A. Morel, O. Napoly and B. Peterson, *Nucl. Phys.* **B190** [**FS3**] (1981) 504.

Figures

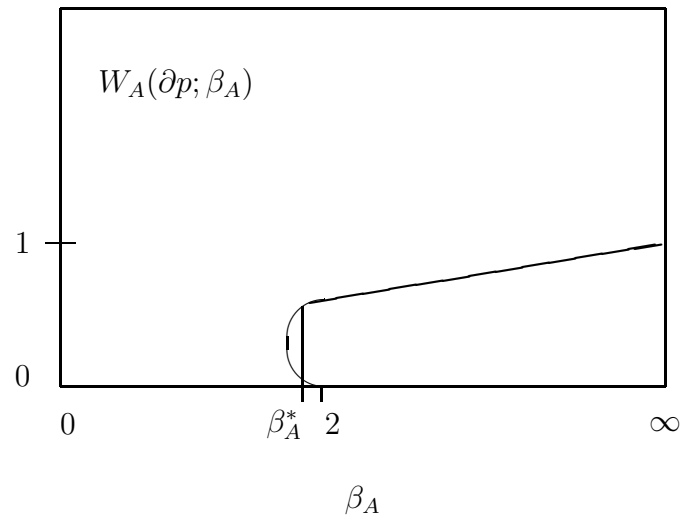


Fig. 1 The two solutions of Eq. (2.15). The line which starts at $\beta_A = 2$ is associated with the solution (2.18). Since the slope is negative for this solution near $\beta_A = 2$ (and $W_A \ll 1$), the first order phase transition occurs at some $\beta_A^* < 2$ so that the actual behavior of $W_A(\partial p; \beta_A)$ is depicted by the bold line.

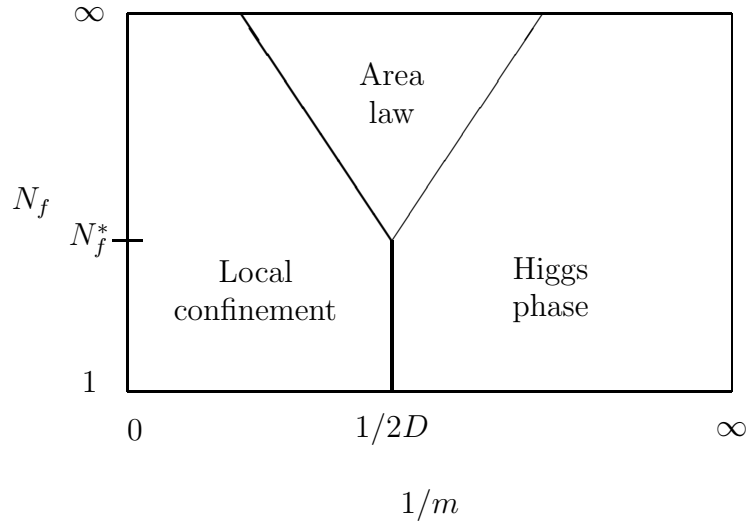


Fig. 2 The mean field prediction for the phase diagram of ASM. The bold lines which bounds the local confinement phase is that of first order phase transitions. The line which separates the area law and Higgs phases is that of second order phase transitions.

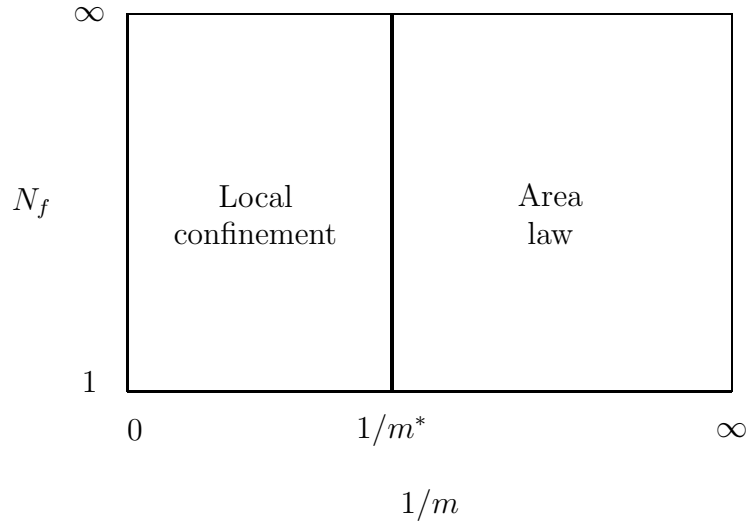


Fig. 3 The mean field prediction for the phase diagram of AFM. The bold line which separates the local confinement and the area law phases is that of first order phase transitions.

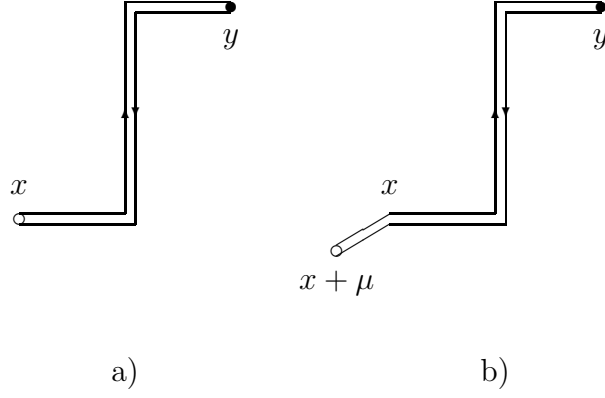


Fig. 4 The graphic representation for $G_\lambda(C_{xy})$ (a) and $G_\lambda(C_{(x+\mu)x}C_{xy})$ (b) entering Eq. (3.2). The empty circles represent $\Phi_f(x)$ or $\Phi_f(x + \mu)$ while the filled ones represent $\frac{1}{\lambda - \Phi_f'(y)}$. The oriented solid lines represent the path-ordered products $U(C_{xy})$ and $U(C_{(x+\mu)x}C_{xy})$. The color indices are contracted according to the arrows.

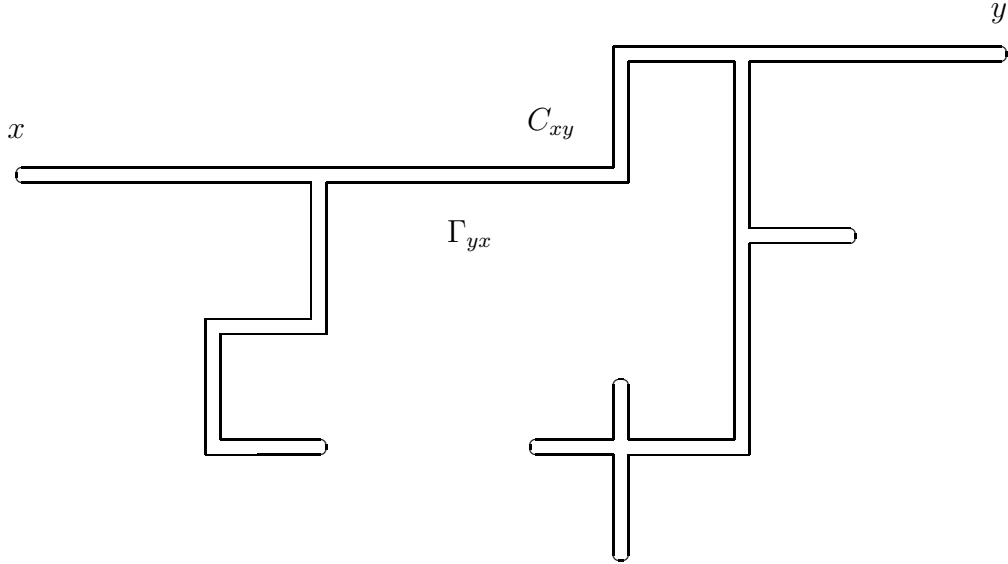


Fig. 5 The typical paths Γ_{yx} which contribute the sum on the r.h.s. of Eq. (3.27) (and Eq. (3.29)). These Γ_{yx} coincide with C_{xy} passed backward modulo backtrackings which form a $1D$ tree. The sum over Γ_{yx} is reduced to summing over the backtrackings.